

doi.org/10.3114/fuse.2023.12.10

## *Plasmopara echinaceae*, a new species of downy mildew affecting cone flowers (*Echinacea purpurea*) in the United States

C. Salgado-Salazar<sup>1\*</sup>, M.K. Romberg<sup>2</sup>, B. Hudelson<sup>3</sup>

<sup>1</sup>Mycology and Nematology Genetic Diversity and Biology Laboratory, U.S. Department of Agriculture, Agriculture Research Service (USDA-ARS), 10300 Baltimore Avenue, Beltsville MD, 20705, USA

<sup>2</sup>National Identification Services, Plant Protection and Quarantine, U.S. Department of Agriculture, Animal and Plant Health Inspection Service (USDA-APHIS), 10300 Baltimore Avenue, Beltsville, MD, 20705, USA

<sup>3</sup>Plant Disease Diagnostics Clinic, Department of Plant Pathology, University of Wisconsin-Madison, 1630 Linden Drive Madison, WI, 53706, USA

\*Corresponding author: Catalina.Salgado@usda.gov

### Key words:

*Asteraceae*  
new taxon  
obligate biotrophs  
*Oomycetes*  
ornamental plants  
*Peronosporaceae*

**Abstract:** Downy mildew is one of the most important diseases of commercial sunflower and other *Asteraceae* hosts, including ornamental *Rudbeckia*. *Plasmopara halstedii* has historically been identified as the causal agent of this disease, considered a complex of species affecting nearly 35 genera in various tribes. However, with the use of molecular DNA characters for phylogenetic studies, distinct lineages of *P. halstedii* in the *Asteraceae* have been identified, confirmed as distinct or segregated as new species. During August of 2022, a downy mildew was observed on potted *Echinacea purpurea* grown in a retail greenhouse in Jefferson County, Wisconsin, USA. Phylogenetic analyses of the cytochrome c oxidase subunit 2 (*cox2*) and nuclear large subunit ribosomal RNA (nc LSU rDNA) gene regions indicated these *Plasmopara* sp. isolates are not conspecific with *P. halstedii*. Based on phylogenetic evidence and new host association, the *Plasmopara* isolates from *E. purpurea* are here described as *Plasmopara echinaceae*. Diagnostic morphological characters for this new species were not observed when compared with other isolates of *P. halstedii* or other *Plasmopara* species found on *Asteraceae* hosts, and therefore a list of species-specific substitutions in the *cox2* region are provided as diagnostic characters. As this study corresponds to the first observation of downy mildew in cone flowers, it is recommended to follow the required disease prevention guidelines to prevent outbreaks and the establishment of this plant pathogen in production sites.

**Citation:** Salgado-Salazar C, Romberg MK, Hudelson B (2023). *Plasmopara echinaceae*, a new species of downy mildew affecting cone flowers (*Echinacea purpurea*) in the United States. *Fungal Systematics and Evolution* 12: 203–217. doi: 10.3114/fuse.2023.12.10

**Received:** 14 June 2023; **Accepted:** 31 August 2023; **Effectively published online:** 22 September 2023

**Corresponding editor:** M. Thines

## INTRODUCTION

The genus *Echinacea* (coneflowers) belongs to the daisy family *Asteraceae* and includes flowering herbaceous perennials. Many are drought-tolerant species. The genus is native and endemic to North America, occurring primarily in the eastern and central US and in southern Canada (Flagel *et al.* 2008). Coneflower plants are also increasingly used in ornamental gardens where they can remain in bloom for long periods of time, are adaptable to a range of soil types and pH and are hardy from U.S.D.A. Zones 3–8 (Baskin *et al.* 1992). The coneflower seedheads attract birds, and the flowers attract multiple pollinator communities, with bees as the most important group (Erickson *et al.* 2021). The species *E. purpurea* or purple coneflower is the most well-known species in the genus *Echinacea*, being widely cultivated as an ornamental (Lim 2014). Other *Echinacea* species also cultivated as ornamentals but to a lesser degree, include *E. angustifolia* (Black samson), *E. pallida* (pale purple coneflower), the endemic and endangered *E. tennesseensis* (Tennessee purple coneflower), and *E. paradoxa* (yellow coneflower). In contrast to

*E. purpurea*, none of these latter species have been developed as ornamentals beyond the wild type (Ault 2007). In addition to their ornamental use, coneflowers have been frequently used as medicinal plants and their preparations are widely used in herbal medicines (Bruni *et al.* 2018). These plants produce large levels of active compounds with different therapeutic uses including treatment of common cold, flu, typhoid, diphtheria, and rheumatoid arthritis as well as various skin problems (Billah *et al.* 2019). For pharmacological applications, the species *E. angustifolia* var. *angustifolia*, *E. pallida* and *E. purpurea* are the most extensively studied and used (Xu *et al.* 2014).

*Echinacea purpurea*, a perennial prairie wildflower and the best-known species, was first described from specimens collected in Virginia (Binns *et al.* 2001, 2002). This species is characterized by erect main stems up to 2 meters in height, alternate leaves on long stalks, coarse hairs, and solitary spiny, reddish orange flowers surrounded by purplish bracts. *Echinacea purpurea* is cultivated widely throughout the United States, Canada, and Europe, especially in Germany, for ornamental uses as well as for its reported medicinal properties (Sharifi-Rad *et al.*

2018). *Echinacea purpurea* is generally considered to have few disease or insect problems; however increased cultivation for both ornamental and pharmaceutical uses can increase the rate at which new and re-emerging diseases are reported. Current diseases of *E. purpurea* are caused mostly by fungi, with a few caused by bacteria, phytoplasmas, viruses, nematodes, and insects (Davenport 2009, Moorman 2016). To date, there are no reports of diseases of *Echinacea* caused by oomycetes, including downy mildews (Farr & Rossman 2023), even though downy mildew diseases are prevalent in many plant genera in the *Asteraceae*. Several genera and species in the *Peronosporaceae* are known to cause downy mildew on host plants in the family *Asteraceae* (Peck 1889, Shaw 1951, Kenneth & Palti 1984, Constantinescu 1996, Voglmayr *et al.* 2004, Constantinescu & Thines 2010, Choi & Thines 2015, Salgado-Salazar *et al.* 2019, Farr & Rossman 2023). Downy mildews in these hosts result in severe economic losses for high value crops due to yield and quality reduction and downgrading of market value. Affected high value crops include oilseed (annual and cultivated sunflowers, *P. halstedii*; Gascuel *et al.* 2015), leafy vegetables (lettuce, *Bremia lactucae*, Spring *et al.* 2018), and ornamental crops (ornamental *Rudbeckia*, *Coreopsis*, *etc.*; Choi *et al.* 2009c, Rivera *et al.* 2016, Salgado-Salazar *et al.* 2019), among others.

In August of 2022, *Echinacea purpurea* (purple coneflowers) with foliar symptoms and signs of downy mildew caused by *Plasmopara* spp. were observed at a retail greenhouse in Jefferson County, Wisconsin, USA. To date, there are no reports of downy mildew on purple coneflower caused by *Plasmopara* or any other downy mildew species in the USA (Farr & Rossman 2023). Traditionally, *P. halstedii* has been designated as causing downy mildew on other species in the *Asteraceae* that are closely related to *Echinacea*. These include commercially important plants such as sunflowers (*Helianthus* sp.), ornamental *Coreopsis* (*Coreopsis* sp.), Black eyed Susan (*Rudbeckia* sp.), Velvet plants (*Gynura* sp.), floss flower (*Ageratum* sp.), among others (Choi *et al.* 2009c, Duarte *et al.* 2013, Palmateer *et al.* 2015, Pisani *et al.* 2019, Rivera *et al.* 2014, 2015, 2016, Salgado-Salazar *et al.* 2019). Since previous studies have found that *P. halstedii* is likely to be an assemblage of many cryptic species (Rivera *et al.* 2016), we used both morphological and molecular phylogenetic approaches to determine if the downy mildew isolates affecting *E. purpurea* were *P. halstedii* or if they constitute an undescribed species.

## MATERIALS AND METHODS

### Sample collection and morphological characterization

*Echinacea purpurea* plants (purple coneflower) showing symptoms and signs of downy mildew disease were observed in a greenhouse in Jefferson County, Wisconsin, USA. A total of five individual plants were examined. Using an entomological pin, sporangial masses were scraped from sporulating lesions on the abaxial leaf surface, mounted in a drop of 85 % lactic acid on a microscope slide and covered with a glass coverslip. Microscope slides were incubated on a warming plate set at 50 °C for 30 min before examination with a Zeiss Axio Imager M2 compound microscope (Zeiss, Jena, Germany). Pieces of leaf tissue with downy mildew lesions (approx. 5 × 5 mm) were examined microscopically for the presence of oospores. Tissue lesions were cleared using a solution of 95 % ethanol-acetic acid-glycerol (75:15:10 v/v) for 2 h or enough time for the tissue to be clear of pigment. Cleared

tissue pieces were placed in 85 % lactic acid on a microscope slide, pressed gently with a cover slip to disrupt tissue, and observed with the compound microscope. Measurements of morphological characters are given as (minimum) – standard deviation towards minimum – average – standard deviation towards the maximum – (maximum) with the number of measurements given in brackets, as recommended by Choi *et al.* (2009b). Additional diseased tissue for all five sample specimens was deposited at the US National Fungus Collection (BPI, Table 1).

### DNA extraction, PCR amplification and sequencing

Extraction of total DNA from leaf samples was performed by excising ca. 10 mm<sup>2</sup> discrete leaf sections colonized by downy mildew structures (mycelia, sporangia) using a sterile razor blade. The plant lesions were homogenized into a fine powder using liquid nitrogen in a sterile ceramic mortar and pestle. DNA was extracted using the E.Z.N.A. HP Fungal DNA Kit (Omega Bio-tek, Inc, Norcross, GA, USA) following the manufacturer's instructions. Amplification products were generated using the primer pairs *cox2*-F/*Cox*-RC4 (*cox2*; Hudspeth *et al.* 2000, Choi *et al.* 2015), *OomCox1*-levup/*OomCox1*-levlo (*cox1*; Robideau *et al.* 2011) LR0R (Vilgalys & Hester 1990) and LR6-O (nLSU rDNA; Riethmüller *et al.* 2002) and ITS1-O (Rouxel *et al.* 2013) and LR-O (nITS rDNA; Moncalvo *et al.* 1995). Amplification reactions were performed in 20 µL volumes containing 10 µL of Platinum™II Hot-Start PCR Master Mix (2X) (Thermo Fisher Scientific, Waltham, MA, USA), 0.4 µL of each primer (10 µM), 5–10 ng of template DNA (1–2 µL), and 7–8 µL of PCR-grade water. Amplification was performed in a C1000 Touch PCR Thermal Cycler (Bio-Rad, Hercules, CA) using PCR cycle conditions described by Salgado-Salazar & Thines (2022). Amplicons were bi-directionally sequenced using a BigDye™ v. 3.1 Terminator Cycle sequencing kit on an Applied Biosystems SeqStudio Genetic Analyzer (Thermo Fisher Scientific, Waltham, MA, USA). Sequences were visually inspected and assembled using CLC Main Workbench v. 23 (QIAGEN, Inc, Germantown, MD, USA).

### Phylogenetic analyses

DNA sequences for *cox2* and LSU markers obtained from the *E. purpurea* specimens, as well as sequence data from related species including those of downy mildew species affecting other hosts in the *Asteraceae* and other plant families, were downloaded from GenBank (Table 1). Individual alignments were obtained using MAFFT v. 7 (<http://mafft.cbrc.jp/alignment/server/>; Katoh & Standley 2013) using the algorithm G-INS-i. The amino acid substitution model best fitting each dataset was estimated using RAxML GUI v. 2.0.10 (Stamatakis 2006, Silvestro & Michalak 2012) based on the Akaike Information Criterion AIC, with GTR+I+G4 identified for *cox2* and LSU. Phylogenetic analyses were run individually for each gene using two different methods. Maximum likelihood (ML) phylogenetic analyses were performed in RAxML GUI v. 2.0.10 (Stamatakis 2006, Silvestro & Michalak 2012) with 1 000 bootstrap replicates. Bayesian inference (BI) phylogenetic trees were obtained using MrBayes v. 3.2.5. Analyses were initiated from random starting trees, run for 10 M generations with four chains (Metropolis-coupled Markov chain Monte Carlo) (Huelsenbeck & Rannala 2004), and sampled every 1 000<sup>th</sup> generations for a total of 10 000 tree samples per run. Default priors were used on all analyses and two independent Bayesian inference (BI) analyses were run. To evaluate stationarity and convergence between runs, log-likelihood

Table 1. List of isolates used in this study.

Species	Isolate number	Host	Country	cox2	LSU	Reference
<i>Plasmopara ampelopsidis</i>	H5	<i>Ampelopsis grandifolia</i> var. <i>brevipedunculata</i>	USA, Maryland	OK631956	OK631721	Salgado-Salazar & Thines (2022)
	H6	<i>Ampelopsis grandifolia</i> var. <i>brevipedunculata</i>	USA, Maryland	OK631957.1	OK631721	Salgado-Salazar & Thines (2022)
<i>Plasmopara angustiterminalis</i>	HOH HUH 674	<i>Xanthium strumarium</i>	Hungary	HM628742.1	n/a	Schroeder et al. (2011)
	KUS-F 24490	<i>Xanthium strumarium</i>	South Korea	MT731364.1	MT729826.1	Lee et al. (2020)
	MTX03A1	<i>Xanthium strumarium</i>	Hungary	HM628741.1	EU826113.1	Schroeder et al. (2011); Goeker (2008)
	SOMF07198	<i>Xanthium strumarium</i>	Bulgaria	EU743812	n/a	Choi et al. (2009b)
<i>Plasmopara australis</i>	Wallace2876	<i>Luffa cylindrica</i>	USA, North Carolina	KT159463.1	KT159461.1	Wallace et al. (2016)
<i>Plasmopara baudysii</i>	H.V. 571	<i>Berula erecta</i>	Austria	EU826098.1	n/a	Voglmayr et al. (2004)
<i>Plasmopara carveri</i>	MI	<i>Vitis riparia</i>	USA, New York	HM628757.1	HM628772.1	Schröder et al. (2011)
	U375	<i>Vitis riparia</i>	USA, Iowa	HM628755.1	n/a	Schröder et al. (2011)
<i>Plasmopara densa</i>	H.V. 2232 (WU)	<i>Rhinanthus alectorolophus</i>	Germany	n/a	EF553464.1	Voglmayr & Constantinescu (2008)
	MG 6-1	<i>Rhinanthus alectorolophus</i>	Germany	DQ365754.1	AY250175.1	Göker et al. (2007); Voglmayr et al. (2004)
<b><i>Plasmopara echinaceae</i> Type</b>	<b>EchDM1/ BPI 911239</b>	<b><i>Echinacea purpurea</i></b>	<b>USA, Wisconsin</b>	<b>OR004814</b>	<b>OR030905</b>	<b>This study</b>
	<b>EchDM2/ BPI 911240</b>	<b><i>Echinacea purpurea</i></b>	<b>USA, Wisconsin</b>	<b>OR004815</b>	<b>OR030906</b>	<b>This study</b>
<i>Plasmopara euphrasiae</i>	WU30283 / H.V. 2226	<i>Euphrasia stricta</i>	Sweden	KF041006.1	EF553465.1	Voglmayr & Constantinescu (2008)
<i>Plasmopara halstedii</i>	AR 179	<i>Flaveria bidentis</i>	Bolivia	n/a	AY178534.1	Spring et al. (2003)
	C1G1	<i>Coreopsis grandifolia</i>	USA, Tennessee	MH807829.1	MH807830.1	Salgado-Salazar et al. (2019)
	C2-hap1	<i>Helianthus annuus</i>	n/a	OM273733.1	n/a	Kitner et al. (2023)
	C2-hap2	<i>Helianthus annuus</i>	n/a	OM273734.1	n/a	Kitner et al. (2023)
	C2-hap3	<i>Helianthus annuus</i>	n/a	OM273735.1	n/a	Kitner et al. (2023)
	C2-hap4	<i>Helianthus annuus</i>	n/a	OM273736.1	n/a	Kitner et al. (2023)
	GynF	<i>Gynura aurantiaca</i>	USA, Florida	n/a	KR028988.1	Palmateer et al. (2015)
	H.V. 921	<i>Helianthus xlaetiflorus</i>	Germany	n/a	AY178529.1	Spring et al. (2003)
	KUS-F 18911	<i>Helianthus annuus</i>	Korea	EU743813.1	EU743803.1	Choi et al. (2009b)
	KUS-F 23701	<i>Coreopsis lanceolata</i>	Korea	n/a	FJ638471.1	Choi et al. (2009c)
	Ph110	<i>Helianthus annuus</i>	Germany	HM628743.1	n/a	Schröder et al. (2011)
	PUL F2909	<i>Ageratum houstonianum</i>	USA, Florida	n/a	KX096708.1	Pisani et al. (2019)
	RDM-FR-1	<i>Rudbeckia fulgida</i> "Goldstrum"	USA, Maryland	n/a	KF927152.1	Rivera et al. (2014)
	RDM1	<i>Rudbeckia fulgida</i> "Goldstrum"	USA, Connecticut	KU232282.1	n/a	Rivera et al. (2016)
	RDM37	<i>Rudbeckia fulgida</i> "Goldstrum"	USA, Maryland	KU232281.1	n/a	Rivera et al. (2016)
	RDM4	<i>Rudbeckia fulgida</i> "Goldstrum"	USA, Ohio	KU232283.1	n/a	Rivera et al. (2016)
	RDM5	<i>Rudbeckia fulgida</i> "Goldstrum"	USA, Maryland	KU232284.1	n/a	Rivera et al. (2016)
	RWB1050	<i>Gerbera jamesonii</i>	Brazil	KC690148.1	n/a	Duarte et al. (2013)
	SDM1	<i>Helianthus annuus</i>	n/a	KU232275.1	n/a	Rivera et al. (2016)

Table 1. (Continued).

Species	Isolate number	Host	Country	cox2	LSU	Reference
	SDM142	<i>Helianthus annuus</i>	n/a	KU232276.1	n/a	Rivera et al. (2016)
	SDM146	<i>Helianthus annuus</i>	n/a	KU232277.1	n/a	Rivera et al. (2016)
	SDM147	<i>Helianthus annuus</i>	n/a	KU232278.1	n/a	Rivera et al. (2016)
	SDM33	<i>Helianthus annuus</i>	USA, North Dakota	KU232280.1	n/a	Rivera et al. (2016)
	SDM74	<i>Helianthus annuus</i>	USA, North Dakota	KU232279.1	n/a	Rivera et al. (2016)
<i>Plasmopara invertifolia</i>	RWB1049	<i>Helichrysum bracteatum</i>	Brazil	KC841910.1	n/a	Duarte et al. (2014)
	RWB975	<i>Helichrysum bracteatum</i>	Brazil	KC841909.1	n/a	Duarte et al. (2014)
<i>Plasmopara majewskii</i>	DAR 69721	<i>Arctotis</i> sp.	Australia	HM628759.1	HQ402933.1	Schröder et al. (2011); Constantinescu & Thines (2010)
	VPRI20080a	<i>Arctotis</i> sp.	Australia	n/a	HQ402932.1	Constantinescu & Thines (2010)
<i>Plasmopara megasperma</i>	MG 39-4	<i>Viola rafinesquii</i>	USA, Tennessee	DQ365755.1	n/a	Göker et al. (2007)
<i>Plasmopara muralis</i>	BPI 911208	<i>Parthenocissus quinquefolia</i>	USA, Maryland	MN807253.1	n/a	Salgado-Salazar & Thines (2022)
	HOH HUH 1024	<i>Parthenocissus tricuspidata</i>	Germany	KJ654170.1	n/a	Choi et al. (2015)
	PmPtL12	<i>Parthenocissus tricuspidata</i>	Poland	MH492326.1	n/a	Mirzwa-Mróz et al. (2019)
<i>Plasmopara nivea</i>	AR 233	<i>Aegopodium podagraria</i>	Germany	n/a	AY250162.1	Voglmayr et al. (2004)
	HOH HUH 586	<i>Aegopodium podagraria</i>	Germany	HM628761.1	n/a	Schröder et al. (2011)
	MG 7-2	<i>Aegopodium podagraria</i>	Germany	DQ365756.1	n/a	Göker et al. (2007)
<i>Plasmopara obducens</i>	H.V. 207	<i>Impatiens noli-tangere</i>	n/a	n/a	EF196869.1	Voglmayr & Thines (2007)
	H.V. 306	<i>Impatiens noli-tangere</i>	n/a	DQ365757.1	n/a	Göker et al. (2007)
	KUS-F 23732	<i>Impatiens walleriana</i>	Korea	n/a	FJ638470.1	Choi et al. (2009a)
<i>Plasmopara pimpinellae</i>	H.V. 634	<i>Pimpinella major</i>	Austria	DQ365758.1	AY035519.2	Göker et al. (2007); Riethmueller et al. (2002)
<i>Plasmopara pusilla</i>	MG 8-10	<i>Geranium pratense</i>	Germany	DQ365759.1	AY035521.2	Göker et al. (2007); Riethmueller et al. (2002)
	WU30280 / H.V. 140	<i>Geranium sibiricum</i>	Austria	n/a	DQ148402.1	Voglmayr et al. (2006)
<i>Plasmopara siegesbeckiae</i>	KUS-F 21312	<i>Siegesbeckia glabrescens</i>	Korea	EU743814.1	EU743805.1	Choi et al. (2009)
<i>Plasmopara</i> sp.	HV-2014a	<i>Plumeria pudica</i>	Austria	KC774622.1	n/a	Voglmayr & Esquivel (2013)
	KUS-F 23331	<i>Ambrosia artemisiifolia</i>	Hungary	EU743820.1	EU743811.1	Choi et al. (2009)
	KUS-F 23333	<i>Ambrosia artemisiifolia</i>	Hungary	EU743819.1	EU743810.1	Choi et al. (2009)
	KUS-F 23334	<i>Ambrosia artemisiifolia</i>	Canada	EU743815.1	EU743806.1	Choi et al. (2009)
	KUS-F 23337	<i>Ambrosia artemisiifolia</i>	USA: Pennsylvania	EU743817.1	EU743808.1	Choi et al. (2009)
<i>Plasmopara sphagnetocolae</i>	BPI 919166	<i>Lipochaeta integrifolia</i>	USA: Hawaii	MT292790.1	n/a	Davis et al. (2020)
	BRIP 61010	<i>Sphagnetocola trilobata</i>	Australia	KM085175.1	KM085176.1	McTaggart et al. (2015)
<i>Plasmopara viticola</i>	MG 11-5	<i>Vitis vinifera</i>	Germany	DQ365760.1	n/a	Göker et al. (2007)
	Pvl	<i>Vitis vinifera</i>	USA: New York	HM628749.1	HM628764.1	Schröder et al. (2011)
	Txl	<i>Vitis vinifera</i>	USA: Texas	HM628748.1	HM628762.1	Schröder et al. (2011)
<i>Plasmoverna pygmaea</i>	AR 86	<i>Anemone ranunculoides</i>	n/a	n/a	AF119605.2	Riethmueller et al. (1999)
	MG 4-6	<i>Anemone ranunculoides</i>	Germany	DQ365761.1	n/a	Göker et al. (2007)



scores were plotted using TRACER v. 1.6 (Rambaut *et al.* 2013). After stationarity evaluation, 25 % of the trees were removed from the analyses. The remaining trees were used to calculate posterior probabilities (PP) and were summarized in a 50 % majority rule consensus tree. Phylogenetic trees were visualized and edited using FigTree v. 1.4.3 (Rambaut 2014). *Plasmoverna pygmaea* was used as outgroup taxon to root the *cox2*, LSU rDNA and concatenated phylogenetic trees (Table 1). Sequence alignments for *cox2* and LSU rDNA datasets, are available through the National Agricultural Library AgData Commons (<https://doi.org/10.15482/USDA.ADC/1529170>).

## RESULTS

### Phylogenetic analyses

The nucleotide sequences generated in this study were deposited in GenBank (Table 1). Sequence data could only be obtained for two out of 5 samples examined. In addition to *cox2* and LSU, the markers *cox1* and ITS were also obtained; however, they were not used for the phylogenetic inference. The *cox1* and ITS sequences were deposited in GenBank (*cox1*: OR004816 & OR004817; ITS: OR031840 & OR031841) to be used as supplementary barcodes for further studies. The *cox2* dataset contained the higher number of taxa as this marker has been extensively used as molecular barcode for oomycetes (Choi *et al.* 2015). The final *cox2* alignment contained 56 taxa including outgroup, consisted of 539 characters of which 310 were conserved, 229 variable and 188 parsimony informative. The final LSU alignment contained 36 taxa including outgroup and consisted of 1 209 characters of which 1 016 were conserved, 191 variable, and 144 parsimony informative. A concatenated *cox2*-LSU dataset using all taxa on Table 1 and a reduced (subset of taxa without missing data) *cox2*-LSU concatenated were also constructed. The concatenated dataset containing all taxa studied consisted of 1 748 characters, of which 1 326 were conserved, 420 variable and 332 parsimony informative. The reduced concatenated dataset contained 23 taxa and consisted of 1 748 characters of which 1 367 were conserved, 379 variable, and 264 parsimony informative.

The best-scoring ML tree topologies obtained from analysis of the *cox2* and LSU datasets are shown in Figs 1 & 2 and includes the branch support values for the ML and BI analyses (bootstrap and posterior probabilities). The phylogenetic reconstructions based on the *cox2* dataset indicated the *Plasmopara* sp. found on *E. purpurea* are not conspecific with *P. halstedii* and/or other species of *Plasmopara* found on *Asteraceae* hosts included in this study, such as *P. angustiterminalis*, *P. majewskii*, *P. invertifolia*, *P. siegesbeckiae* and *P. sphagneticola*. Specimens of *Plasmopara* on *E. purpurea* form a separate, well supported clade, closely related to *P. australis*, although this relationship lacks significant branch support (Fig. 1). The phylogenetic reconstruction using the LSU dataset showed the isolates from *E. purpurea* form a well-supported, monophyletic clade and are closely related to *P. halstedii* and *P. sphagneticolae*, as opposed to what was observed for the *cox2* dataset (Fig. 2). An isolate of *P. halstedii* on *Flaveria bidentis* appears as sister single isolate lineage to *Plasmopara* on *E. purpurea* (Fig. 2). The phylogenetic analyses of the concatenated *cox2*-LSU dataset produced trees with well supported terminal lineages, including specimens of *Plasmopara* on *E. purpurea* (Figs 3, 4).

The concatenated *cox2*-LSU dataset with and without missing data showed the same general relationships and support among *Plasmopara* species, although branch supports obtained from the analysis of combined dataset without missing data showed better resolution for interior nodes in the phylogenies (Fig. 4). The individual *cox2* and LSU phylogenies, as well as those of concatenated *cox2*-LSU datasets, show *Plasmopara* species found on *Asteraceae* hosts do not form a monophyletic group, and are distributed throughout the tree (Figs 3, 4).

### Disease symptoms and morphological characterization

Symptoms of downy mildew were investigated in a total of five affected plants (BPI numbers 911239, 911240, 911241, 911242, 911243). However, the microscopic observation of morphological features of the purple coneflower downy mildew pathogen (Fig. 5) were based on samples taken from two of the specimens showing disease signs, *i.e.*, active abaxial sporulation (specimens BPI 911239 holotype and BPI 911240). The remaining specimens showed only initial symptoms of the disease without any signs of the pathogen. Plants affected by the downy mildew show symptoms on the upper side of the leaves, including foliar vein delimited lesions that start as chlorotic spots, later turning dark brown due to necrosis (Fig. 5). As disease progresses, necrotic leaf lesions coalesce causing complete necrosis of leaves. White downy growth can be observed on the lower surface of the leaves, with active sporulation observed during the initial stages prior to necrosis. In necrotic tissues, the downy growth of the pathogen turned dark brown or completely dislodged from the leaf tissue (Fig. 5).

*Plasmopara* isolates on *E. purpurea* showed sporangiophore lengths ranging from 219–460  $\mu\text{m}$  (291.8–)325.4–378.1–430.8(–460.4)  $\mu\text{m}$ , and (6.5–)7.4–9.3–11.2(–12.5)  $\mu\text{m}$  width at the base (av. 378.1  $\times$  9.3  $\mu\text{m}$ ,  $n = 103$ ). These sporangiophores were monopodially branched with terminal branchlets at right angles, (5.9–)7.2–8.8–10.4(–12)  $\mu\text{m}$  in length (av. 8.8  $\mu\text{m}$ ,  $n = 61$ ). The observed sporangia sizes ranged from (17.4–)19.8–23.9–28(–34.3)  $\times$  (12.6–)15.5–18.4–21.3(–24.8)  $\mu\text{m}$ , L/W ratio (0.9–)1.2–1.3–1.5(–1.7), (av. 23.9  $\times$  18.4  $\mu\text{m}$ ,  $n = 77$ , Fig. 5). The isolates here designated as *P. echinaceae* sp. nov. showed no significant morphological variations to those included in the *P. halstedii* protologue (sporangiophores 300–750  $\mu\text{m}$  long and 11–15  $\mu\text{m}$  width at the base, sporangia 19–30  $\mu\text{m}$  long, and 16–26  $\mu\text{m}$  wide, av. 24.5  $\times$  20.5  $\mu\text{m}$ ) (Saccardo 1888). No differences were observed also for *P. halstedii* isolates found on other plants in the tribes *Arctotideae*, *Eupatorieae*, *Heliantheae* and *Mutisieae* (Table 2), for example *P. halstedii* on *Ageratum houstonianum* (Pisani *et al.* 2019), *Coreopsis* sp. (Choi *et al.* 2009c, Salgado-Salazar *et al.* 2019), *Gerbera jamesonii* (Duarte *et al.* 2013), *Gynura aurantica* (Palmateer *et al.* 2015), *Helianthus  $\times$ laetiflorus*, and *Rudbeckia fulgida* (Rivera *et al.* 2014, 2015). Based on the phylogenetic analyses of single genes and combined datasets, the species *P. australis* on *Luffa cylindrica* and *P. halstedii* on *F. bidentis* are closely related to the *Plasmopara* isolates on *E. purpurea*. No information about morphological characters could be found for *Plasmopara* on *F. bidentis* (Spring *et al.* 2003), and *P. australis* shows smaller sporangia when compared to those of *Plasmopara* on *E. purpurea*. Related to other species of *Plasmopara* found on other *Asteraceae* hosts, *P. angustiterminalis* (Lee *et al.* 2020), *P. invertifolia* (Duarte *et al.* 2014), *P. siegesbeckia* (Lee *et al.* 2020), and *P. sphagneticolae* (McTaggart *et al.* 2015), seem to be the only species showing morphological differences by producing sporangia smaller than those of *Plasmopara* from *E. purpurea* or *P. halstedii* on other *Asteraceae* hosts (Table 2) (see Notes in Taxonomy section).

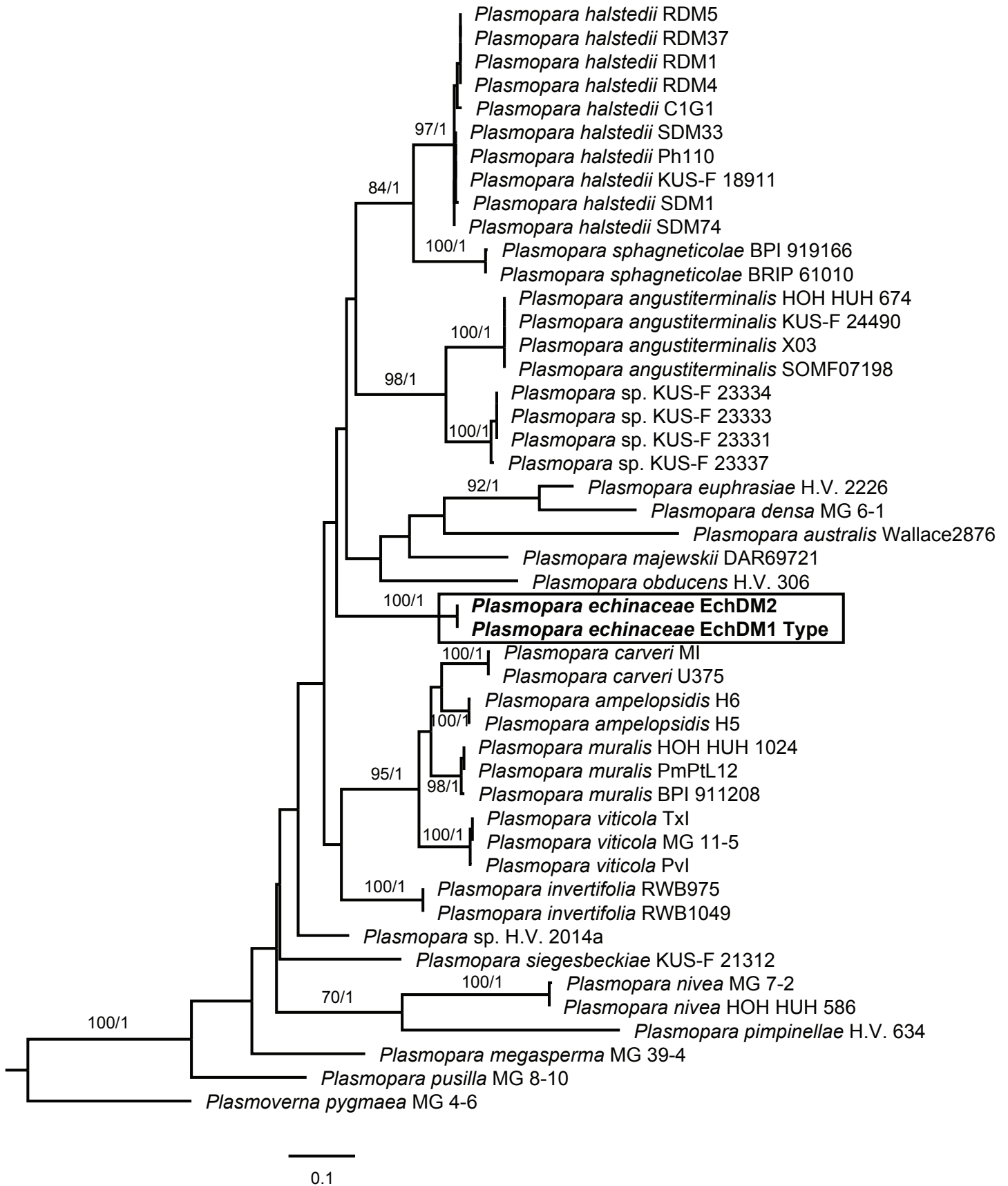


**Fig. 1.** Phylogenetic reconstruction (ML, BI) based on the *cox2* sequence data. Support values (bootstrap and posterior probabilities) are indicated above branches (ML/BI). Lack of support value indicates the branch was not supported at values higher than 0.95 PP, and 70% bootstrap. *Plasmoverna pygmaea* was used as outgroup.

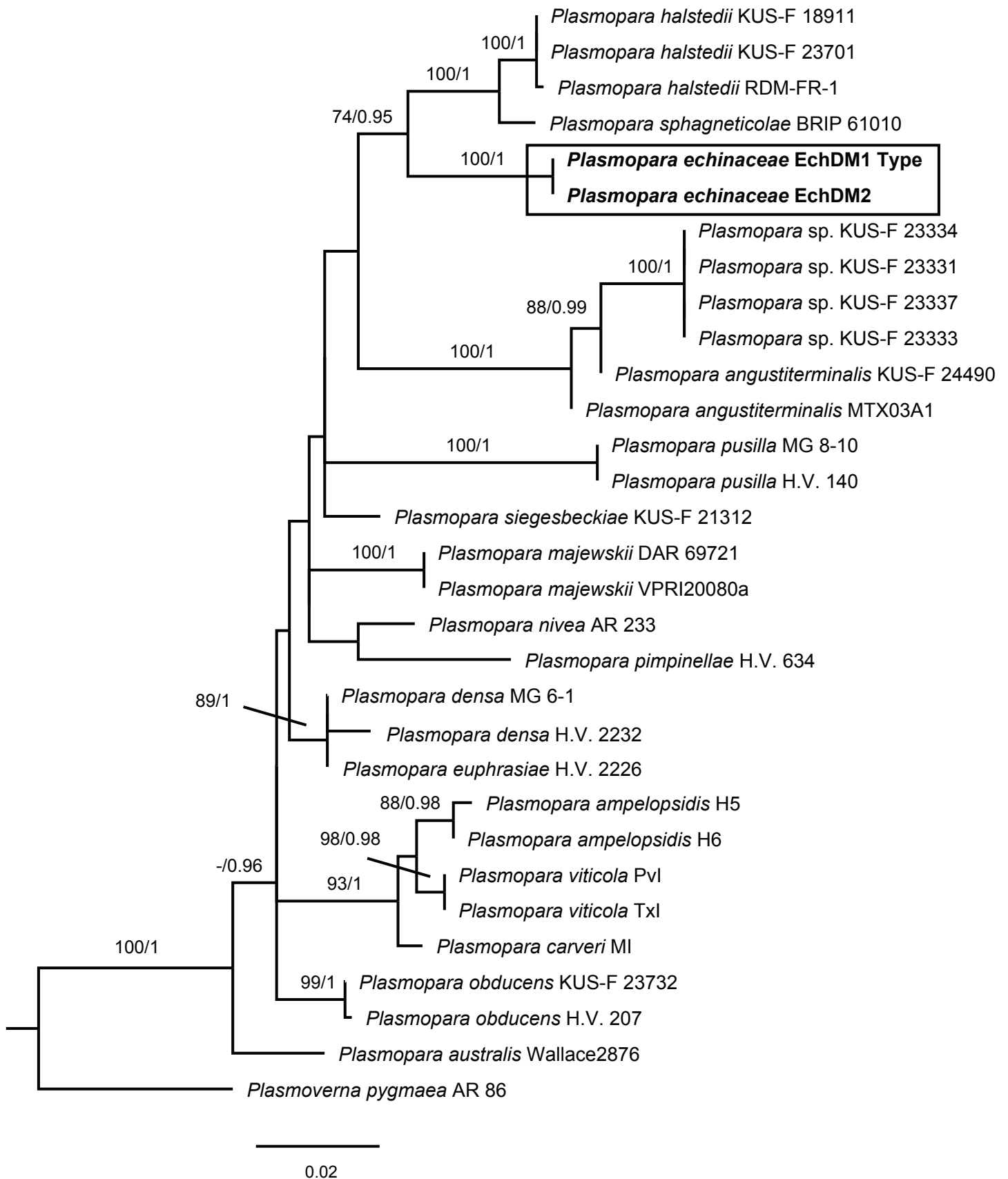


**Fig. 2.** Phylogenetic reconstruction (ML, BI) based on the LSU sequence data. Support values (bootstrap and posterior probabilities) are indicated above branches (ML/BI). Lack of support value indicates the branch was not supported at values higher than 0.95 PP, and 70 % bootstrap. *Plasmoverna pygmaea* was used as outgroup.

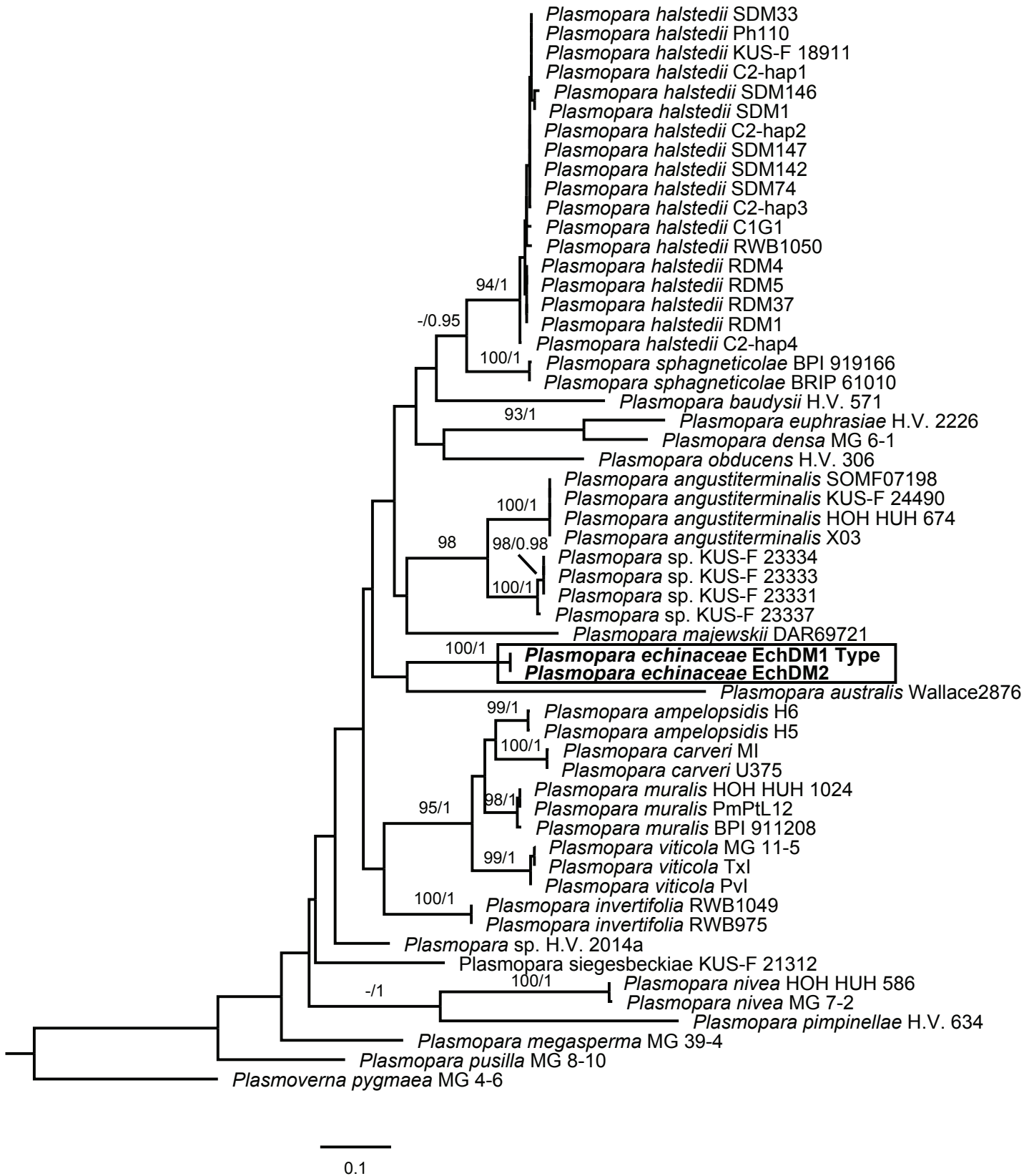


**Fig. 3.** Phylogenetic reconstruction (ML, BI) based on the *cox2* – LSU concatenated analysis with missing data. Support values (bootstrap and posterior probabilities) are indicated above branches (ML/BI). Lack of support value indicates the branch was not supported at values higher than 0.95 PP, and 70 % bootstrap. *Plasmoverna pygmaea* was used as outgroup.



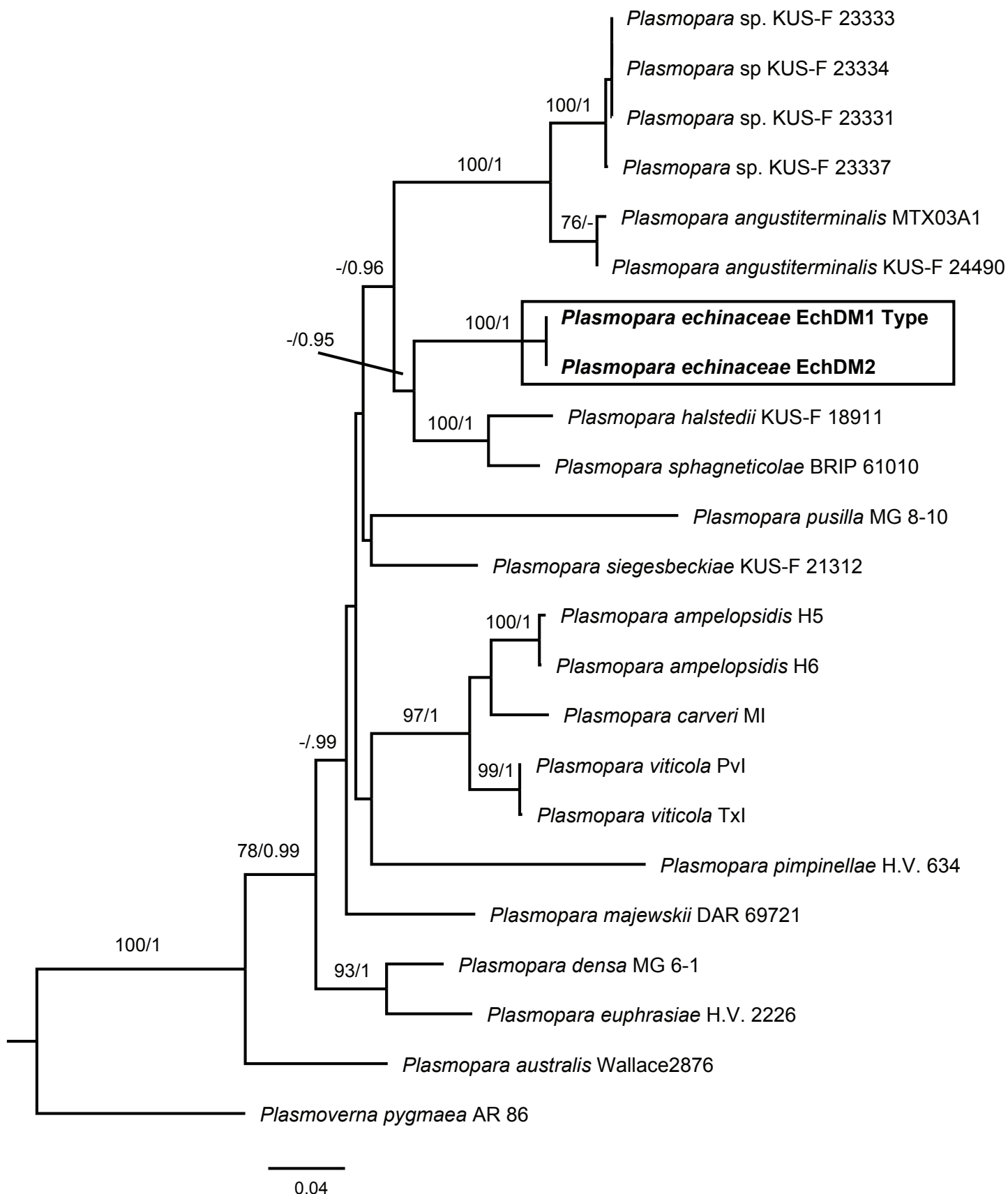


**Fig. 4.** Phylogenetic reconstruction (ML, BI) based on the *cox2* – LSU reduced concatenated sequence data. Support values (bootstrap and posterior probabilities) are indicated above branches (ML/BI). Lack of support value indicates the branch was not supported at values higher than 0.95 PP, and 70 % bootstrap. *Plasmoverna pygmaea* was used as outgroup.

**Table 2.** Comparative measurements of sporangiophores and sporangia from *Plasmopara halstedii* and other *Plasmopara* species on Asteraceae hosts.

Species (host species)	Sporangiophores	Sporangia	Reference
<i>Plasmopara echinaceae</i> ( <i>Echinacea purpurea</i> )	291–460 µm, base 6.5–12.5 µm	19–28 × 15–21 µm (av. 23–18 µm)	This study
<i>Plasmopara halstedii</i> (Protologue)	300–750 µm, base 11–15 µm	19–30 × 15–26 µm (av. 24–20 µm)	Saccardo (1888)
<i>Plasmopara halstedii</i> ( <i>Helianthus laetiflorus</i> )	450–700 µm, base 8–12 µm	av. 25 × 20 µm	Spring et al. (2003)
<i>Plasmopara halstedii</i> ( <i>Rudbeckia fulgida</i> )	261–904 µm, base n/a	av. 24 × 20 µm	Rivera et al. (2014, 2015)
<i>Plasmopara halstedii</i> ( <i>Ageratum houstonianum</i> )	Up to 550 µm, base 8.5–14.4 µm	16–24 × 12–18 µm (av. 20–15 µm)	Pisani et al. (2019)
<i>Plasmopara halstedii</i> ( <i>Coreopsis grandiflora</i> )	344–579 µm, base 7–13 µm	15–22 × 13–19 µm (av. 18–16 µm)	Salgado-Salazar et al. (2019)
<i>Plasmopara halstedii</i> ( <i>Coreopsis lanceolata</i> )	350–500 µm, base 7–13.5 µm	19–26 × 16–21 µm (av. 22–20 µm)	Choi et al. (2009c)
<i>Plasmopara halstedii</i> ( <i>Gerbera jamesonii</i> )	Up to 650 µm, base 6.5–13 µm	20–28 × 13–18 µm (av. 24–20 µm)	Duarte et al. (2013)
<i>Plasmopara halstedii</i> ( <i>Gynura aurantica</i> )	n/a	21–29 × 17–21 µm (av. 25–19 µm)	Palmateer et al. (2015)
<i>Plasmopara angustiterminalis</i> ( <i>Xanthium</i> sp.)	200–550 µm, base 6–10 µm	19–22 × 13–15 µm (av. 20–14 µm)	Lee et al. (2020)
<i>Plasmopara invertifolia</i> ( <i>Helichrysum bracteatum</i> )	Up to 670 µm, base 7.5–12 µm	9–20 × 9–18 µm (av. 14–13 µm)	Duarte et al. (2014)
<i>Plasmopara majewskii</i> ( <i>Arctotis</i> sp., Type)	360–650 µm, base up to 13 µm	20–27 × 16–22 µm (av. 23–19 µm)	Constantinescu & Thines (2010)
<i>Plasmopara siegesbeckia</i> ( <i>Siegesbeckia glabrescens</i> )	150–550 µm, base up to 11 µm	18–22 × 13–16 µm (av. 20–14 µm)	Lee et al. (2020)
<i>Plasmopara spagneticolae</i> ( <i>Spagneticola trilobata</i> , Type)	300–50 µm, base 7–13 µm	15–27 × 14–20 µm (av. 21–17 µm)	McTaggart et al. (2015)
<i>Plasmopara spagneticolae</i> ( <i>Lipochaeta integrifolia</i> )	n/a	15–24 × 12–19 µm (av. 19–15 µm)	Davis et al. (2020)
<i>Plasmopara</i> sp. ( <i>Ambrosia artemisiifolia</i> )	220–490 µm, base up to 15 µm	19–26 × 15–19 µm (av. 22–17 µm)	Choi et al. (2009)
<i>Plasmopara</i> aff. <i>australis</i> ( <i>Luffa cylindrica</i> )*	348–771 µm, base 8–16 µm	13–18 × 11–15 µm (av. 15–13 µm)	Wallace et al. (2016)
<i>Plasmopara baudysii</i> ( <i>Berula erecta</i> )*	90–250 µm, base 8–12 µm	21–31 × 17–21 µm (av. 26–19 µm)	Skalicky (1954)

\* not on Asteraceae.

## Taxonomy

Based on the phylogenetic analyses of two molecular markers, morphological data, and host distribution, we describe here a new *Plasmopara* species infecting *Echinacea purpurea* (Purple cone flower).

***Plasmopara echinaceae*** C. Salgado & B. Hudelson, *sp. nov.* MycoBank MB 849048. Fig. 5.

**Etymology:** The name refers to the genus of the host plant where this species can be found (*Echinacea purpurea*).

**Typus:** USA, Wisconsin, Jefferson County, on leaves of *Echinacea purpurea* in greenhouse retailer, Aug. 2022, B. Hudelson UWPDDC-1475/EchDM1 (**holotype** BPI 911239).

**Diagnosis:** *Plasmopara echinaceae* has only been found on *E. purpurea*. Additionally, it can be diagnosed by the following species-specific nucleotide characters, which are fixed in *cox2* sequences between *P. echinaceae* and other downy mildew species on *Asteraceae*, including *P. halstedii* on various hosts, *P. angustiterminalis*, *P. invertifolia*, *P. majewskii*, *P. siegesbeckia*, *P. sphagnetocolae*, *Plasmopara* sp. on *Ambrosia*, by positions 39 (G:A), 129 (A:T), 235 (C:T), 237 (G:A), 300 (C:T), 304 (T:C), 312 (A:T), 347 (T:C/A), 396 (G:A/T), 435 (C:T), 489 (T:A/C). This alignment is available through the National Agricultural Library AgData Commons (<https://doi.org/10.15482/USDA.ADC/1529170>).

**Description:** *Sporangiophores* emerging through stomata, hyaline, straight or slightly curved, 219–460 length × 6–12 µm width at the base (av. 378.1 × 9.3 µm); basal end of sporangiophore not differentiated to slightly bulbous, callose plugs often present. Branches straight, monopodial. Ultimate branchlets 2–3 base not inflated or slightly swollen, diverging at 70–90° angle, 8.8 µm length on average. *Sporangia* subglobose to broadly ellipsoidal, hyaline, 17.4–34.3 µm length × 12.6–24.8 µm width (av. 23.9 × 18.4 µm), L/W ratio 0.9–1.7, sporangia tip round or slightly apiculate; covered by a lenticular or outwardly convex papilla. *Sexual structures* (oospores) not seen.

**Additional specimen examined:** USA, Wisconsin, Jefferson County, on leaves of *Echinacea purpurea*, August 2022, B. Hudelson EchDM2 (BPI 911240).

**Host:** *Echinacea purpurea*.

**Geographic distribution:** USA, Wisconsin.

**Barcodes:** *cox2*: OR004814, OR004815; LSU: OR030905, OR030906. Additional molecular markers *cox1*: OR004816, OR004817; ITS: OR031840, OR031841.

**Notes:** Phylogenetic analyses of *cox2* and LSU datasets showed *P. echinaceae* is genetically close to *P. australis* and *P. baudysii*. However, these species are known to cause disease in members of the families *Cucurbitaceae* and *Apiaceae*, respectively. This, together with the provided single nucleotide polymorphisms in the *cox2* gene, can distinguish *P. echinaceae* from these downy mildew species, as well as from others found on other *Asteraceae* hosts. The *cox2* alignment used to define the species-specific

nucleotides is deposited at USDA AgData Commons (<https://doi.org/10.15482/USDA.ADC/1529170>).

## DISCUSSION

The molecular differences and new host information indicated the presence of a separate and new species on the *Asteraceae* species *Echinacea purpurea*, here named *Plasmopara echinaceae*. Traditionally, downy mildew pathogens occurring on several hosts in the *Asteraceae* were initially labeled as *P. halstedii*, however, phylogenetic and population genetic studies carried out in the last 20 years (e.g., Spring *et al.* 2003, 2006, Choi *et al.* 2009b, Rivera *et al.* 2016) have shown that *P. halstedii* is a complex of cryptic species. Even though advocacy for the split of *P. halstedii* into several species has existed for many decades (Novotel'nova 1962a, b, 1963), only the inclusion of molecular data in phylogenetics has allowed researchers to understand and correctly apply species limits in this group. Examples of independent lineages in *P. halstedii sensu lato* segregated into distinct species include *P. angustiterminalis* on *Xanthium* spp., *P. invertifolia* on *Helichrysum bracteatum*, *P. majewskii* on *Arctotis × hybrida*, and *P. sphagnetocolae* on *Spagneticola trilobata*, among others. Despite the segregation of some lineages into different species, *P. halstedii* as of now still shows a wide range host that includes plants in the subtribes *Eupatorieae*, *Heliantheae*, *Millieriae*, and *Mutisieae* (Choi *et al.* 2009c, Duarte *et al.* 2013, Rivera *et al.* 2014, 2015, Palmateer *et al.* 2015, Pisani *et al.* 2019, Salgado-Salazar *et al.* 2019).

*Plasmopara halstedii sensu lato* and other *Plasmopara* species found on *Asteraceae* are examples of morphologically conservative species. In this study we observed that sizes of morphological characters showed no significant differences among species of *Plasmopara* affecting this host family. Morphology is strongly linked to functional demands, which are in turn dependent on the environment. Consequently, lack of significant morphological variation is considered a strong indicator of the specific ecological preferences and function of downy mildew species (Voet *et al.* 2022). In this study we could observe that published sizes of morphological characters among different *P. halstedii* isolates and among other *Plasmopara* species found on *Asteraceae*, do not have enough size variation to allow individuals to be identified based on morphology. Kulkarni *et al.* (2009) reported in a comparative analysis of the sizes of various morphological characters in *P. halstedii* that isolates displaying virulence differences, did not show significant differences in sporangiophore length and sporangia size, as these showed overlapping values, and slight differences were due to intraspecific variation. Lack of morphological characters used for systematic studies has required the incorporation of single nucleotide polymorphisms at mitochondrial DNA gene regions, phylogenetic divergence, and host association as species delimiting characters.

Systematic and taxonomic studies of downy mildew species in the *Peronosporaceae* are increasing with the purpose of verifying taxonomic entities, updating nomenclature, and establishing species limits, especially for species groups previously described using only comparative morphology. Even after this renewed interest, molecular DNA data to be used in phylogenetic studies is still scarce in data repositories like GenBank, where either most data found is restricted to one gene or is specifically abundant for isolates of species which detrimental effect in



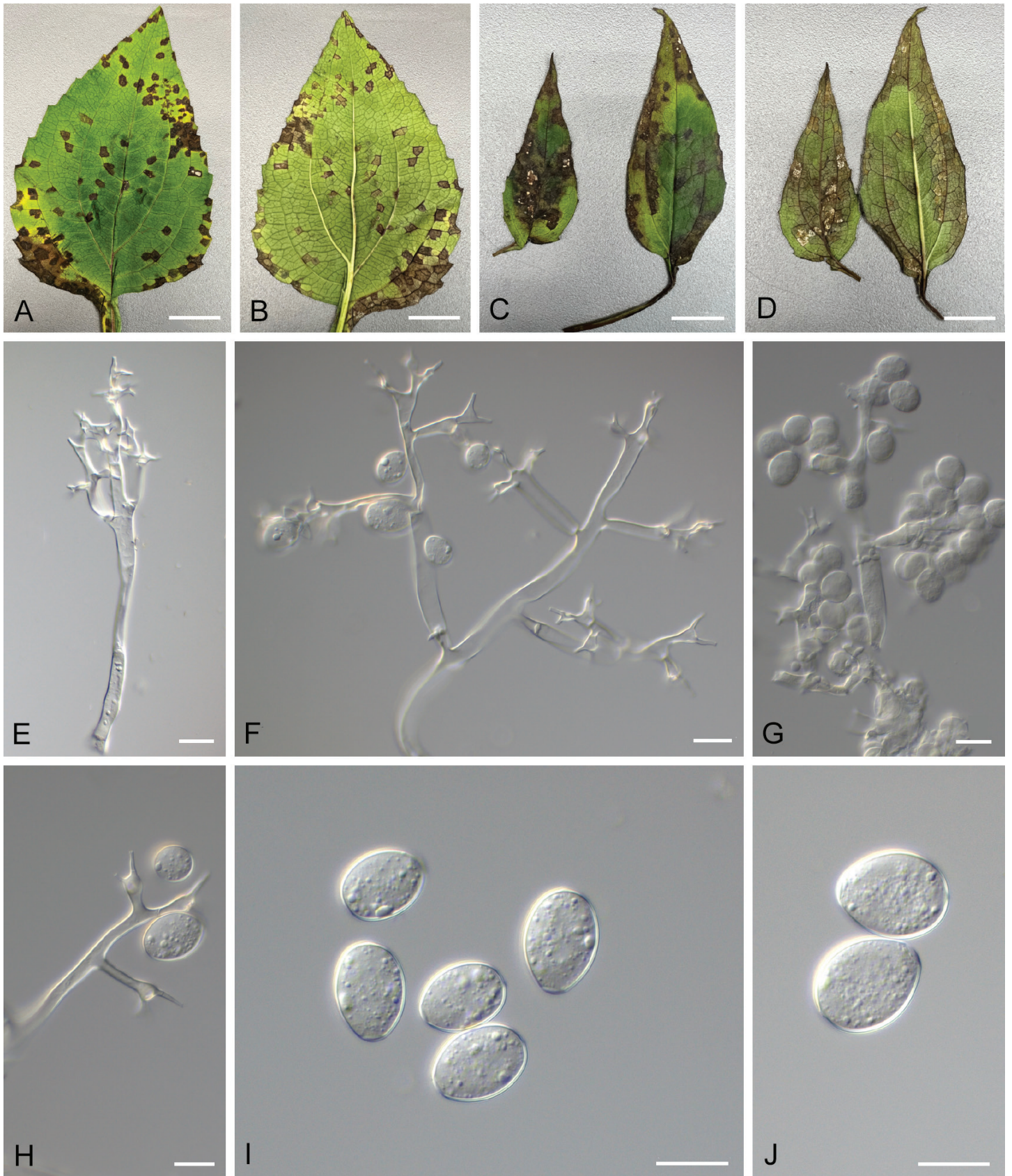


**Fig. 5.** Symptoms and signs of downy mildew affecting *Echinacea purpurea*. **A–D.** Diseased leaves displaying vein delimited, dark brown spots surrounded by chlorotic tissues around lesions. **E, F.** Sporangiophores. **G, H.** Close-up image of sporangiophore ramifications showing sporangia developing and ultimate branchlets. **I, J.** Sporangia. Scale bars: A–D = 1 cm; E–J = 20 μm.



agriculture has high economic impact (*i.e.*, *Plasmopara viticola*, *P. halstedii* on sunflower, *Pseudoperonospora cubensis*). Due to this limitation, multi-locus phylogenetic analysis of species of certain genera or host groups would require the introduction of missing data in the phylogenetic analysis. Still, it is important to include in this kind of studies species for which there is little to no data. In this study, the introduction of missing data in the multilocus analysis, or the analysis of a reduced multi-locus did not have an effect in the designation of the *Plasmopara* isolates on *E. purpurea* as new species. We also observed that not all *Plasmopara* species found on *Asteraceae* hosts cluster in the same group or have a single common ancestor, which is the case for *P. invertifolia*. We could also observe that *Plasmopara* species not found on *Asteraceae* hosts, such as *P. baudysii*, clustered in the main group containing *P. halstedii*, *P. angustiterminalis*, and *P. sphagneticola*. Consequently, based on previous and current studies, the evolutionary origin of downy mildew species on *Asteraceae*, patterns of species diversification, and species relationships remain unresolved.

Downy mildew diseases caused by *Plasmopara* species are some of the most severe and destructive diseases of ornamental plants, impacting the quality of product, making it a major constraint for the ornamental industry. Herbaceous perennial plants remain popular for its use in private gardens and in commercial landscapes in the United States, and it was estimated that the value of herbaceous perennials for wholesale operations with \$100 000+ in sales in 36 selected states within the U.S. was estimated to be \$4.63 billion for 2018, compared with \$4.37 billion for 2015. Production in California and Florida account for 46 percent of the total value and the number of producers for 2018 was up 8 % compared with 2015 (Source: USDA - NASS Floriculture Crops 2018 Summary, May 2019). Downy mildew species particularly affect the floriculture and ornamental plants industry, especially those grown under protected environments (greenhouses). In these conditions, downy mildews can be common and can cause significant economic losses, by reducing yield and quality of crops and downgrading the value of ornamentals (Daughtrey & Benson 2005). Delimiting and describing new species of downy mildews and recording their current and new geographical distribution is fundamental for the study of emergent and re-emergent threats to agricultural, horticultural, or natural ecosystems. Taxonomic knowledge has a direct impact on epidemiological studies (spore trapping, disease survey and weather monitoring), and facilitates the development of integrated pest management and a predictive model for downy mildew occurrence on horticultural crops.

## ACKNOWLEDGEMENTS

This work was supported by funds from USDA-ARS project 8042-22000-298-00-D. Mention of trade names or commercial products in this publication is solely for the purpose of providing specific information and does not imply recommendation or endorsement by the USDA. The USDA is an equal opportunity provider and employer.

**Conflict of interest:** The authors declare that there is no conflict of interest.

## REFERENCES

- Ault JR (2007). Coneflower. In: *Flower Breeding and Genetics* (Anderson NO, ed.). Springer, Dordrecht: 801–824.
- Baskin CC, Baskin JM, Hoffman GR (1992). Seed dormancy in the prairie forb *Echinacea angustifolia* var. *angustifolia* (Asteraceae): after ripening pattern during cold stratification. *International Journal of Plant Sciences* **153**: 239–243.
- Billah MdM, Hosen MdB, Khan F, et al. (2019). *Echinacea*. Chapter. 3.13 In: *Nonvitamin and Nonmineral Nutritional Supplements* (Nabavi SM, Silva AS, eds.). Academic Press: 205–210.
- Binns SE, Baum BR, Arnason JT (2001). Typification of *Echinacea purpurea* (L.) Moench (*Heliantheae*: *Asteraceae*) and implications for the correct naming of two *Echinacea* taxa. *Taxon* **50**: 1169–1175.
- Binns SE, Baum BR, Arnason JT (2002). A taxonomic revision of *Echinacea* (*Asteraceae*: *Heliantheae*). *Systematic Botany* **27**: 610–632.
- Bruni R, Brighenti V, Caesar LK, et al. (2018). Analytical methods for the study of bioactive compounds from medicinally used *Echinacea* species. *Journal of Pharmaceutical and Biomedical Analysis* **160**: 443–477.
- Choi Y-J, Beakes G, Glockling S, et al. (2015). Towards a universal barcode of oomycetes – a comparison of the *cox1* and *cox2* loci. *Molecular Ecology Resources* **15**: 1275–1288.
- Choi YJ, Han JG, Park MJ, et al. (2009a). Downy mildew of *Impatiens balsamina* and *I. walleriana* in Korea. *The Plant Pathology Journal* **25**: 433.
- Choi YJ, Kiss L, Vajna L, et al. (2009b). Characterization of a *Plasmopara* species on *Ambrosia artemisiifolia*, and notes on *P. halstedii*, based on morphology and multiple gene phylogenies. *Mycological Research* **113**: 1127–1136.
- Choi YJ, Park MJ, Shin HD (2009c). First Korean report of downy mildew on *Coreopsis lanceolata* caused by *Plasmopara halstedii*. *Plant Pathology* **58**: 1171.
- Choi YJ, Thines M (2015). Host jumps and radiation, not co-divergence drives diversification of obligate pathogens. A case study in downy mildews and *Asteraceae*. *PLoS ONE* **10**: e0133655.
- Constantinescu O (1996). *Paraperonospora apiculata* sp. nov. *Sydowia* **48**: 105–110.
- Constantinescu O, Thines M (2010). *Plasmopara halstedii* is absent from Australia and New Zealand. *Polish Botanical Journal* **55**: 293–298.
- Davenport M (2009). *Echinacea*. Clemson Cooperative Extension, Home and Garden Information Center. Available at: <https://hgic.clemson.edu/factsheet/echinacea/>
- Daughtrey ML, Benson DM (2005). Principles of plant health management for ornamental plants. *Annual Review of Phytopathology* **43**: 141–169.
- Davis WJ, Ko M, Ocenar, JR, et al. (2020). First report of *Plasmopara sphagneticolae* on the native Hawaiian plant *Lipochaeta integrifolia*. *Australasian Plant Disease Notes* **15**: 29.
- Duarte LL, Choi Y-J, Barreto RW (2013). First report of downy mildew caused by *Plasmopara halstedii* on *Gerbera jamesonii* in Brazil. *Plant Disease* **97**: 1382–1382.
- Duarte LL, Choi Y-J, Soares DJ, et al. (2014). *Plasmopara invertifolia* sp. nov. causing downy mildew on *Helichrysum bracteatum* (*Asteraceae*). *Mycological Progress* **13**: 285–289.
- Erickson E, Patch HM, Grozinger CM (2021). Herbaceous perennial plants can support complex pollinator communities. *Scientific Reports* **11**: 17352.
- Farr DF, Rossman AY (2021). *Fungal Databases, U.S. National Fungus Collections, ARS, USDA*. Retrieved March 13, 2021, from <https://nt.ars-grin.gov/fungaldbases/>



- Flagel LE, Rapp RA, Grover CE, *et al.* (2008). Phylogenetic, morphological, and chemotaxonomic incongruence in the North American endemic genus *Echinacea*. *American Journal of Botany* **95**: 756–765.
- Gascuel Q, Martinez Y, Boniface M-C, *et al.* (2015). *Plasmopara halstedii*, sunflower downy mildew. *Molecular Plant Pathology* **16**: 109–122.
- Göker M, Voglmayr H, Riethmüller A, *et al.* (2007). How do obligate parasites evolve: A multi-gene phylogenetic analysis of downy mildews. *Fungal Genetics and Biology* **44**: 105–122.
- Huelsenbeck JP, Rannala B (2004). Frequentist properties of Bayesian posterior probabilities of phylogenetic trees under simple and complex substitution models. *Systematic Biology* **53**: 904–913.
- Hudspeth DSS, Nadler SA, Hudspeth MES (2000). A *cox2* molecular phylogeny of the *Peronosporomycetes*. *Mycologia* **92**: 674–684.
- Katoh K, Standley DM (2013). MAFFT multiple sequence alignment software version 7: improvements in performance and usability. *Molecular Biology and Evolution* **30**: 772–780.
- Kenneth RG, Palti J (1984). The distribution of downy and powdery mildews and of rusts over tribes of *Compositae* (*Asteraceae*). *Mycologia* **76**: 705–718.
- Kitner M, Thines M, Sedlarova M, *et al.* (2023). Genetic structure of *Plasmopara halstedii* populations across Europe and South Russia. *Plant Pathology* **72**: 361–375.
- Kulkarni S, Hegde YR, Kota RV (2009). Pathogenic and morphological variability of *Plasmopara halstedii*, the causal agent of downy mildew in sunflower. *Helia* **32**: 85–90.
- Lee JS, Shin HD, Choi Y-J (2020). Rediscovery of seven long-forgotten species of *Peronospora* and *Plasmopara* (*Oomycota*). *Mycobiology* **48**: 331–340.
- Lim TK (2014). *Echinacea purpurea*. In: *Edible Medicinal and Non-Medicinal Plants*. Springer, Dordrecht.
- McTaggart AR, Shuey LS, McKenna SG, *et al.* (2015). *Plasmopara sphagneticolae* sp. nov. (*Peronosporales*) on *Sphagneticola* (*Asteraceae*) in Australia. *Australasian Plant Pathology* **44**: 81–85.
- Mirzwa-Mróz E, Kukuła W, Kuźma K, *et al.* (2019). First report of downy mildew caused by *Plasmopara muralis* on Boston Ivy (*Parthenocissus tricuspidata*) in Poland. *Plant Disease* **103**: 1793.
- Moncalvo J-M, Wang H-H, Hseu R-S (1995). Phylogenetic relationships in *Ganoderma* inferred from the Internal Transcribed Spacers and 25S Ribosomal DNA sequences. *Mycologia* **87**: 223–238.
- Moorman GW (2016). *Echinacea* diseases. PennState Extension. Available at: <https://extension.psu.edu/echinacea-diseases>
- Novotel'nova NS (1962a). K woprosu o loznoj muc'nistoj rose podsolnec'nika [Downy mildew on sunflowers]. *Sbornik Dokla dov Nauc'noj Konferencii po Zas'c'ita Rastenij* (Tallinn): 129–138.
- Novotel'nova NS (1962b). *Plasmopara halstedii* as a composite species (the basis for the taxonomic division of the genus *Plasmopara* on *Compositae*). *Botanicheskii Zhurnal* **47**: 970–981.
- Novotel'nova NS (1963). Nowye widy *Plasmopara* na *Compositae*. *Botanic'eskie materialy Otdela sporvykh rastenij Botanicheskogo instituta Akademii nauk SSSR* **16**: 72–83.
- Rambaut A (2014). *FigTree v. 1.4.3*. <http://tree.bio.ed.ac.uk/software/figtree/>
- Rambaut A, Suchard M, Drummond A (2013). *Tracer v. 1.6*. <http://tree.bio.ed.ac.uk/software/tracer/>
- Palmateer AJ, Cating RA, Lopez P (2015). First report of downy mildew on *Gynura aurantiaca* by *Plasmopara halstedii sensu lato* in Florida. *Plant Disease* **99**: 1279.
- Peck CH (1889). Report of the Botanist. In: *Annual Report of the Regents*: 74. Albany, J.B. Lyon, State Printer, 1890–1903.
- Pisani C, Patel PC, Roskopf EN, *et al.* (2019). First report of downy mildew caused by *Plasmopara halstedii* on *Ageratum houstonianum* in the United States. *Plant Disease* **103**: 2968.
- Riethmüller A, Voglmayr H, Göker M, *et al.* (2002). Phylogenetic relationships of the downy mildews (*Peronosporales*) and related groups based on nuclear large subunit ribosomal DNA sequences. *Mycologia* **94**: 834–849.
- Riethmüller A, Weiss M, Oberwinkler F (1999). Phylogenetic studies of *Saprolegniomycetidae* and related groups based on nuclear large subunit ribosomal DNA sequences. *Canadian Journal of Botany* **77**: 1790–1800.
- Rivera Y, Creswell TC, Ruhl G, *et al.* (2015). First report of downy mildew caused by *Plasmopara halstedii* on native *Rudbeckia fulgida* Aiton var. *speciosa* (Wender.) Perdue in Indiana. *Plant Disease* **99**: 1278–1278
- Rivera Y, Rane K, Crouch JA (2014). First report of downy mildew caused by *Plasmopara halstedii* on Black-eyed Susan (*Rudbeckia fulgida* cv. 'Goldstrum') in Maryland. *Plant Disease* **98**: 1005.
- Rivera Y, Salgado-Salazar C, Gulya T, *et al.* (2016). Emergent rudbeckia downy mildew epidemics caused by *Plasmopara halstedii* are genetically distinct from the pathogen populations infecting sunflower. *Phytopathology* **106**: 752–761.
- Robideau GP, De Cock AW, Coffey MD, *et al.* (2011). DNA barcoding of oomycetes with cytochrome c oxidase subunit I and internal transcribed spacer. *Molecular Ecology Resources* **11**: 1002–1011.
- Rouxel M, Mestre P, Baudoin A, *et al.* (2014). Geographic distribution of cryptic species of *Plasmopara viticola* causing downy mildew on wild and cultivated grape in Eastern North America. *Phytopathology* **104**: 692–701.
- Rouxel M, Mestre P, Comont G, *et al.* (2013). Phylogenetic and experimental evidence for host-specialized cryptic species in a biotrophic oomycete. *New Phytologist* **197**: 251–263.
- Saccardo PA (1888). *Sylloge Fungorum Omnium Hucusque Cognitorum Digessit* **7**: 242.
- Salgado-Salazar C, Creswell TC, Ruhl G, *et al.* (2019). First report of *Plasmopara halstedii* on *Coreopsis grandiflora* in the United States. *Plant Disease* **103**: 775.
- Salgado-Salazar C, Thines M (2022). Two new species of *Plasmopara* affecting wild grapes in the United States. *Mycological Progress* **21**: 63.
- Schröder S, Telle S, Nuck P, *et al.* (2011). Cryptic diversity of *Plasmopara viticola* (*Oomycota*, *Peronosporaceae*) in North America. *Organisms Diversity and Evolution* **11**: 3–7.
- Sharifi-Rad M, Mnayer D, Bezerra Morais-Braga MF, *et al.* (2018). *Echinacea* plants as antioxidant and antibacterial agents: From traditional medicine to biotechnological applications. *Phytotherapy Research* **32**: 1653–1663.
- Silvestro D, Michalak I (2012). raxmlGUI: a graphical front-end for RAxML. *Organisms Diversity and Evolution* **12**: 335–337.
- Skalicky V (1954). Studies on the parasitic family *Peronosporaceae* II: New *Plasmopara* species of the phylogenetic compass of the species *Plasmopara umbelliferarum*. *Ceska Mykologie* **8**: 176–179.
- Shaw CG (1951). New Species of the *Peronosporaceae*. *Mycologia* **43**: 445–455.
- Spring O, Bachofer M, Thines M, *et al.* (2006). Intraspecific relationship of *Plasmopara halstedii* isolates differing in pathogenicity and geographic origin based on ITS sequence data. *European Journal of Plant Pathology* **114**: 309–315.
- Spring O, Gomez-Zeledon J, Hadziabdic D, *et al.* (2018). Biological characteristics and assessment of virulence diversity in pathosystems of economically important biotrophic oomycetes. *Critical Reviews in Plant Sciences* **37**: 439–495.
- Spring O, Voglmayr H, Riethmüller A, *et al.* (2003). Characterization of a *Plasmopara* isolate from *Helianthus x laetiflorus* based on cross infection, morphology, fatty acid and molecular phylogenetic data. *Mycological Progress* **2**: 163–170.

- Stamatakis A (2006). RAxML-VI-HPC: maximum likelihood-based phylogenetic analyses with thousands of taxa and mixed models. *Bioinformatics* **22**: 2688–2690.
- Vilgalys R, Hester M (1990). Rapid genetic identification and mapping of enzymatically amplified ribosomal DNA from several *Cryptococcus* species. *Journal of Bacteriology* **172**: 4238–4246.
- Voet I, Denys C, Colyn M, *et al.* (2022). Incongruences between morphology and molecular phylogeny provide an insight into the diversification of the *Crocidura poensis* species complex. *Scientific Reports* **22**: 10531.
- Voglmayr H, Constantinescu O (2008). Revision and reclassification of three *Plasmopara* species based on morphological and molecular phylogenetic data. *Mycological Research* **112**: 487–501.
- Voglmayr H, Fatehi J, Constantinescu O (2006). Revision of *Plasmopara* (*Chromista*, *Peronosporales*) parasitic on *Geraniaceae*. *Mycological Research* **110**: 633–645.
- Voglmayr H, Riethmüller A, Göker M, *et al.* (2004). Phylogenetic relationships of *Plasmopara*, *Bremia* and other genera of downy mildew pathogens with pyriform haustoria based on Bayesian analysis of partial LSU rDNA sequence data. *Mycological Research* **108**: 1011–1024.
- Voglmayr H, Thines M (2007). Phylogenetic relationships and nomenclature of *Bremiella sphaerosperma* (*Chromista*, *Peronosporales*). *Mycotaxon* **100**: 11–20.
- Wallace E, Choi YJ, Thines M, *et al.* (2016). First report of *Plasmopara* aff. *australis* on *Luffa cylindrica* in the United States. *Plant Disease* **100**: 537.
- Xu CG, Tang TX, Chen R, *et al.* (2014). A comparative study of bioactive secondary metabolite production in diploid and tetraploid *Echinacea purpurea* (L.) Moench. *Plant Cell, Tissue and Organ Culture* **116**: 323–332.